15. J. C. Yarnold, *ibid.* **105**, 345 (1993).
16. L. Muller, *Rock Mech. Eng. Geol.* **6**, 1 (1968).
17. B. Voight and W. Pariseau, in *Geotechnical Engineering*, B. Voight, Ed. (Elsevier, Amsterdam, 1978), pp. 1–67.
18. R. Lopes *et al.*, *J. Geophys. Res.* **87**, 9917 (1982); R. Lopes *et al.*, *Moon Planets* **22**, 221 (1980); P. W. Francis and G. Wadge, *J. Geophys. Res.* **88**, 8333 (1983); M. Bulmer and P. McGovern, *Lunar Planet. Sci.*, in press.
19. R. Dingle, *J. Geol. Soc. London* **134**, 293 (1977); C. Summerhayes *et al.*, *Mar. Geol.* **31**, 265 (1979).
20. See P. Schenk and M. Bulmer [*Lunar Planet Sci.* **XXVIII**, 1247 (1997)] and M. Bulmer (in preparation), and references therein.
21. The average friction coefficient is given by the tangent of the slope connecting the pre- and postevent centers of gravity of a failed mass (*30*). Because it is not possible to determine the pre- and postevent centers of gravity for masses on Io or most other planets, we use the tangent of the slope angle of the line connecting the top of the scarp to the toe of the apron (*13*) to derive the ratio *H*:*L*. The value derived using this method approximates the center of gravity gradient for those slope failures whose center of gravity lies near the toe (*10*), which may be the case for Euboea. Taking these caveats into consideration, we use *H*:*L* as an estimate of the coefficient of friction.
22. M. H. Bulmer and J. E. Guest, in *Volcano Instability on the Earth and Other Planets*, W. J. McGuire, A. P. Jones, J. Neuberg, Eds. (Geological Society of London, London, 1996), p. 349.
23. At 16 km height, Boosaule Montes (10°S, 270°W) is the highest mountain identified to date on Io. The automated stereogrammetry (*5*) measurement we report has been confirmed by manual measurement of parallax in the Voyager images.
24. Previous estimates that the crust of Io is ~30 km thick (*31*) assumed that mountain heights are due to isostatic buoyancy of material that is lower in density than the surrounding crust. Our interpretation of the formation of Euboea Montes suggests that mountains may have the same density as the surrounding crust, indicating that these crustal thickness estimates are not generally relevant to Io.
25. R. Allmendinger, in *Geology of North America—An Overview*, vol. G-3 of *Geology of North America*, B. Burchfiel, P. Lipman, M. Zoback, Eds. (Geological Society of America, Boulder, CO, 1992), pp. 583–608; D. Miller, T. Nilsen, W. Bilodeau, *ibid.*, pp. 205–260.
26. T. Jordan and R. Allmendinger, *Am. J. Sci.* **286**, 737 (1986).
27. S. Smithson *et al.*, *J. Geophys. Res.* **84**, 5955 (1979).
28. On Io, it is not known whether such faults penetrate the crust or the lithosphere.
29. R. Lopes-Gautier *et al.*, *Geophys. Res. Lett.* **24**, 2439 (1997); M. Carr, paper presented at the Lowell Observatory during the Galileo Era Conference, Flagstaff, AZ, 22 to 24 September 1997.
30. D. Cruden, *Geol. Soc. Am. Bull.* **91**, 63 (1980).
31. D. Nash *et al.*, in *Satellites*, J. Burns and M. Matthews, Eds. (Univ. of Arizona Press, Tucson, AZ, 1986), pp. 629–688.
32. This report is Lunar and Planetary Contribution No. 940. This work was done while M.H.B. was a Garber Fellow at the National Air and Space Museum. We are grateful to J. Moore, W. McKinnon, and an anonymous reviewer for comments.

31 October 1997; accepted 27 January 1998

Single-Grain ^{40}Ar-^{39}Ar Ages of Glauconies: Implications for the Geologic Time Scale and Global Sea Level Variations

Patrick E. Smith, Norman M. Evensen, Derek York, Gilles S. Odin

The mineral series glaucony supplies 40% of the absolute-age database for the geologic time scale of the last 250 million years. However, glauconies have long been suspected of giving young potassium-argon ages on bulk samples. Laser-probe argon-argon dating shows that glaucony populations comprise grains with a wide range of ages, suggesting a period of genesis several times longer (~5 million years) than previously thought. An estimate of the age of their enclosing sediments (and therefore of time scale boundaries) is given by the oldest nonrelict grains in the glaucony populations, whereas the formation times of the younger grains appear to be modulated by global sea level.

Glaucony (*1*) is an authigenic, millimeter-sized, greenish grain of marine clay consisting of aggregates of micrometer-sized crystallites. It is the only mineral facies that is sufficiently widespread to provide direct K-Ar and Rb-Sr ages for sediments. Glaucony is important for calibrating the geologic time scale because it provides ages in strata lacking reliable high-temperature chronometers (*2*), but glaucony ages have also been regarded as untrustworthy (*3*) because they are commonly too young. Glauconies are variable in composition because of a complicated authigenic evolution on the sea floor (*4*). Isotopic study indicated that immature, K-poor glauconies make poor chronometers, whereas evolved K-rich glauconies (>7 weight % K_2O) make the best dating material (*5*).

Glauconies used in the construction of modern time scales have undergone careful selection criteria (*6*). Although direct comparison of evolved glauconies to high-temperature minerals in a single well-understood stratigraphic section has not been possible, and although some high-temperature minerals may give anomalously old ages (*7*), slightly younger ages are apparent for time scales calibrated using glauconies (*7*) relative to scales constructed exclusively with high-temperature minerals (*8*). Consequently, some workers have chosen to ignore glauconies altogether in constructing their time scales. However, this strategy is unfortunate because glaucony is widespread in the geologic record and typically allows superior stratigraphic control.

The ability to date individual grains of glaucony by the ^{40}Ar-^{39}Ar method (*9*) allowed us to reexamine the use of glauconies for dating sediments. We investigated the uniformity of ages in three evolved bulk samples used to construct the geologic time scale (*10*), with K-Ar ages of about 20, 40, and 95 million years ago (Ma). For the single-grain dating, we used the technique of microencapsulation (*11*) to overcome the problem of loss of ^{39}Ar by recoil during irradiation (*9*). In parallel with the glauconies, we tested the reproducibility of 49 single grains of the sanidine age monitor Taylor Creek Rhyolite (TCR), which has crystal sizes small enough to yield individual age variances similar to those of the glauconies. The age distribution for TCR (Fig. 1) is singly peaked with a mean of 27.92 ± 0.05 Ma (*12*).

In contrast, the age distributions of the glauconies have multiple peaks (Fig. 1) with age ranges of ≳5 Ma (*13*). The color variations and wide ranges of ^{39}Ar recoil losses in the populations indicate that these samples contain grains that have been variably glauconitized, but there is no conspicuous relation between these parameters and a grain's age (Table 1). The question of which (if any) of the grains from a given population provide the best estimate of sedimentation age can only be answered by comparing their ages with presumably reliable and correlatable high-temperature mineral ages.

Each glaucony sample is taken from immediately above a stage boundary in the time scale. In each case, therefore, we can compare the ages of these samples to a set of high-temperature mineral ages drawn from rocks immediately below the same stratigraphic boundary (Fig. 1). The high-temperature minerals comprise all the ages in Harland *et al.*'s database (*14*) for the appropriate stages (Albian, Lutetian, and Aquitanian). The broad age distributions of these high-temperature minerals reflect not

P. E. Smith, N. M. Evensen, D. York, Department of Physics, University of Toronto, 60 St. George Street, Toronto, Ontario M5S 1A7, Canada.
G. S. Odin, Département de Géologie Sédimentaire, Université P. et M. Curie, 4 Place Jussieu, Case 119A, 75252 Paris Cedex 05, France.

only their experimental uncertainties, but also a stratigraphic uncertainty associated with their unknown positions within their stages (*15*).

For each of the three age comparisons, the distributions for the glauconies are younger than their respective high-temperature mineral distributions with minimal age overlap (Fig. 1). There is therefore negligible evidence for inherited radiogenic Ar contributed by relict substrates (*16*). The close (≤2 Ma) proximity of the older edge of each glaucony curve to the younger edge of the respective high-temperature mineral curve indicates that the oldest glauconies of a population provide reasonable estimates of their stage boundaries. Using an appropriate statistical treatment (*17*) on each glaucony–high-temperature mineral data set gives $20.5^{+2.6}_{-2.5}$ Ma for the Burdigalian-Aquitanian, $43.4^{+2.9}_{-1.7}$ Ma for the Bartonian-Lutetian, and $96.7^{+3.1}_{-2.7}$ Ma for the Cenomanian-Albian stage boundaries. These are in agreement, within uncertainties, with literature ages (*14*) of 23.1 ± 0.8 Ma, $43.8^{+2.9}_{-2.3}$ Ma, and $97.7^{+2.2}_{-3.4}$ Ma, respectively, using only high-temperature minerals for both overlying and underlying stages.

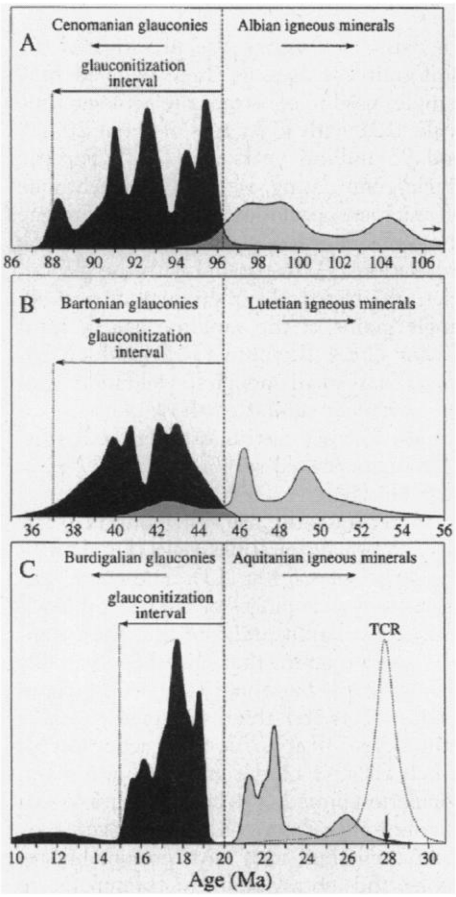

Fig. 1. ^{40}Ar-^{39}Ar age distributions of single glauconies (dark shading) compared with those for high-temperature minerals from the underlying stage [(*14*), light shading], all normalized to a single scale. (**A**) Glaucony GL-O (high-temperature distribution continues to the right of plot); (**B**) glaucony 132a; (**C**) glaucony 385a. Also shown is the distribution for TCR sanidine (reduced to 20% vertical scale); arrow indicates accepted age of TCR (*12*). Dashed vertical lines between glaucony and high-temperature distributions represent visual estimates of the stage boundaries. Length of glauconitization interval is approximate (all uncertainties 1σ).

Table 1. Summary of ^{40}Ar-^{39}Ar data for single glauconies ($^{40}Ar^*$, radiogenic Ar). All glauconies were smooth-textured except for suspected relict grains (†). Abbreviations for evolved grains: bl, black; dg, dark green; g, green. Abbreviations for less evolved to immature grains: mg, mid-green; lg, light green. Data are corrected for mass discrimination, Ca-derived neutron-generated Ar isotopes, and a ^{40}Ar blank (1×10^{-12} to 2×10^{-12} cm^3) at standard temperature and pressure. ^{40}K decay constant $\lambda_{tot} = 5.543 \times 10^{-10}$ year^{-1}. All glaucony ages were calculated by integrating the recoiled ^{39}Ar in the ampoule with the data from the residual grain, except for GL-O8-8 where ampoule gas was run with fused grain. Uncertainties are given at 1σ.

Sample	Color	^{39}Ar recoil loss (%)	$^{40}Ar^*$ (%)	Integrated age (Ma)
385a100	g	29.5	26.9	11.7 ± 1.6
385a101	g	20.3	38.9	15.5 ± 0.3
385a104	g	19.7	30.0	16.2 ± 0.3
385a125	g	28.8	48.7	16.7 ± 0.5
385a109	g	20.8	62.8	17.0 ± 0.3
385a103	g	20.0	65.9	17.6 ± 0.3
385a120	g	18.9	48.8	17.7 ± 0.4
385a97	g	20.9	36.0	17.8 ± 0.2
385a123	g	19.1	59.5	18.0 ± 0.2
385a105	g	19.9	71.2	18.3 ± 0.2
385a121	g	19.5	67.7	18.8 ± 0.2
385a122	g	19.2	37.9	18.9 ± 0.2
385a127	g†	19.6	30.9	25.6 ± 0.5
132a4-17	bl	14.9	94.2	43.9 ± 0.9
132a8-33	bl	16.4	89.1	42.9 ± 0.4
132a8-32	bl	17.5	91.2	42.1 ± 0.3
132a4-18	dg	19.6	90.6	43.0 ± 0.8
132a8-37	dg	18.6	87.2	40.0 ± 0.4
132a8-39	dg	18.9	87.4	40.8 ± 0.3
132a4-19	mg	21.0	76.9	38.2 ± 1.3
132a4-20	lg	29.4	54.7	40.6 ± 1.8
132a8-43	lg	22.0	78.6	39.1 ± 0.8
132a8-44	lg	27.9	65.3	43.7 ± 0.9
GL-O4-12	bl	14.5	95.0	92.4 ± 0.6
GL-O8-l	bl	15.1	96.1	94.7 ± 0.3
GL-O8-2	bl	13.6	97.1	95.4 ± 0.2
GL-O8-3	bl	15.1	88.6	95.6 ± 0.3
GL-O8-4	bl	16.7	90.9	91.1 ± 0.2
GL-O8-5	bl	17.4	95.8	91.3 ± 0.8
GL-O8-46	bl	22.0	94.1	93.1 ± 0.7
GL-O4-13	dg	14.3	96.6	92.9 ± 0.4
GL-O8-7	dg	14.9	96.1	94.4 ± 0.3
GL-O8-6	dg	18.5	93.2	92.6 ± 0.3
GL-O8-8	dg		58.9	95.8 ± 0.3
GL-O4-14	dg†	16.2	97.0	99.2 ± 0.5
GL-O4-15	g	19.5	94.8	90.3 ± 0.9
GL-O4-16	lg	24.9	86.9	88.3 ± 0.4
GL-O8-18	lg	29.7	87.7	94.5 ± 2.2

The spread of the data for glauconies in each population is toward younger ages (*18*). Although some young ages for immature grains may reflect postburial Ar loss (*19*), the more robust evolved glauconies are also frequently too young and by themselves account for most of the age variation in each population (Table 1). It is possible that these young grains were subjected to prolonged or renewed glaucony genesis. The timing of geochemical closure of glaucony, when the grain ceases to exchange K or Ar with the enclosing sediment, is not well known. Closure in immature grains may occur upon burial, whereas for evolved grains closure is reached before burial, when the grains attain 8.5 to 9.0% K_2O, and is completed within an estimated 10^5 to 10^6 years (*6*). However, the more extended (>4 Ma) period implied for the younger grains suggests one or more additional periods of evolution.

If the three populations studied here are representative, the use of single-grain ^{40}Ar-^{39}Ar techniques on glauconies used to calibrate the time scale should increase their ages by 1 to 3 Ma relative to their K-Ar ages, as indicated from the age difference between the oldest (nondetrital) grains and their respective population means (*20*). Currently, the dominant source of error in Cenozoic time scales, which use interpolation of high-temperature mineral ages to obtain boundary ages, is the uncertainty of the stratigraphic position of the dated unit relative to the boundary. Application of single-grain glaucony ^{40}Ar-^{39}Ar dating should increase the number of stratigraphic units that can be reliably dated, and because glaucony often occurs in sediments containing correlatable fossil assemblages, this dating offers the potential for reducing the stratigraphic uncertainty in geologic time scales.

The glauconitization process is modulated by depth to the sea-sediment interface (*6*, *21*), and therefore the continued evolution of grains may reflect changes in sea level after the initial glauconitization period. Because glauconitization is favored during transgressive periods, hiatuses in the glaucony age distributions could reflect times of interrupted glauconitization during regressions. The hiatuses at 41.5 Ma for the Bartonian samples (Fig. 1B) and 93.5 Ma for the Cenomanian samples (Fig. 1A) correspond to major episodes of low sea level on the short-term eustatic sea level curve of Haq *et al.* (*22*). This raises the possibility that the record of 5 Ma of global sea level variation is encoded in the detailed glaucony age distributions from a single sample site. ^{40}Ar-^{39}Ar dating of single glauconies to precisely calibrate global sea level would be important to oil exploration and stratigraphic analysis, where hypothesized globally synchronous sea level cycles form the basis of the popular paradigm of sequence stratigraphy.

REFERENCES AND NOTES

1. As opposed to the specific layered-silicate mineral glauconite, the term "glaucony" is used as a facies term for the family of marine Fe-rich minerals ranging in composition from glauconitic smectite to glauconitic mica.
2. G. J. Wasserburg, R. J. Hayden, J. Jensen, *Geochim. Cosmochim. Acta* **10**, 153 (1956).
3. See, for example, J. D. Obradovitch, *Paleoceanography* **3**, 757 (1988).
4. G. S. Odin, Ed., *Green Marine Clays* (Elsevier, Amsterdam, 1988).
5. ———, Ed., *Numerical Dating in Stratigraphy* (Wiley-Interscience, New York, 1982), part 1, pp. 151–454.
6. ———, *ibid.*, pp. 387–403.
7. ———, *C. R. Acad. Sci. Paris* **318**, 59 (1994).
8. W. A. Berggren, D. V. Kent, J. J. Flynn, J. A. Van Couvering, *Geol. Soc. Am. Bull.* **96**, 1407 (1985).
9. Recoil loss of ^{39}Ar previously prohibited the application of ^{40}Ar-^{39}Ar ages to clay minerals. The problem was overcome by use of a grain encapsulation technique [P. E. Smith, N. M. Evensen, D. York, *Geology* **21**, 41 (1993)].
10. Samples: 385a (K-Ar age = 20.5 ± 0.5 Ma); 132a (K-Ar age = 40.8 ± 1.3 Ma); and GL-O (K-Ar age = 95.0 ± 0.6 Ma, 1σ). Mineralogy and stratigraphy are as described in (*5*).
11. Standard and sample grains were placed in pure quartz tubing (diameter, 1 mm) and attached to a quartz manifold evacuated to a pressure of ~10^{-8} torr. Each sample tube was hand-held while heating the top to detach the ampoule from the manifold, ensuring minimal sample heating. Ampoules were loaded together with flux monitors of Hb-3gr hornblende (assumed age, 1071 Ma) in capsules and irradiated for 24 hours (48 MWh) in position 5C of the McMaster Nuclear Reactor, Hamilton, Ontario. Recoiled Ar gas associated with each sample was measured after breaking the ampoule under high vacuum using a custom-designed crushing apparatus and admitting the released gas into a high-sensitivity mass spectrometer. The grain was then fused using a 20-W continuous Ar-ion laser to measure Ar remaining in the sample. Our experiments have not detected any radiogenic ^{40}Ar leakage from the grain to the ampoule before or during irradiation. Therefore, all glaucony ages were calculated by integrating the recoiled ^{39}Ar in the ampoule with the data from the residual grain.
12. The uncertainty is the standard error of the mean. The age distributions represent the point-by-point sum of the probability densities of each individual age analysis. Although the curves for each age analysis have equal area, more precisely determined ages give more pronounced spikes, whereas ages with higher uncertainties appear as broader, lower-amplitude deflections. A quantitative measure of the degree to which n individual ages are scattered in a population, taking into account their individual experimental uncertainties, is given by $S/(n-1)$, where S is the sum of squares of the weighted deviates about the mean age. This has an expected value of 1 for a data set where no significant age variability can be detected. The value of this quantity for TCR is 0.96, indicating that we have detected no significant age variation of this standard within the limits of our experimental procedure. The weighted mean age is identical to the currently accepted age of 27.92 Ma for this standard [A. Baksi, *Eos* **73**, 328 (1992)].
13. The $S/(n-1)$ values of 6.2 for 385a, 2.8 for 132a, and 6.9 for GL-O confirm that significant age variability exists in the three populations.
14. W. B. Harland *et al.*, *A Geological Time Scale 1989* (Cambridge Univ. Press, Cambridge, 1989).
15. The high-temperature minerals are derived worldwide from any level within that stage, an interval of 4 Ma or more.
16. Older ages of 25.6 ± 0.4 Ma for 385a and 99.2 ± 0.5 Ma for GL-O (Table 1) from grains having anomalously rough surface textures suggest an extraformational origin.
17. A. Cox and G. D. Dalrymple, *J. Geophys. Res.* **72**, 2603 (1967).
18. The conventional K-Ar method requires tens of milligrams of sample, comprising thousands of glaucony grains, for adequate analytical precision and to obtain representative aliquots for separate K analysis. The wide range of single-grain ages for the glaucony populations shows that such multigrain ages [including all those in the Harland *et al.* database (*14*)] must average heterogeneous grains with distinct histories and thus have limited precise significance. Furthermore, because the majority of grains in these populations are significantly younger than the depositional age of their host sediments, the averages tend to be young, which provides an explanation for the age biases in glaucony K-Ar ages used to construct the geologic time scale. (Even heterogeneous age distributions will yield reproducible K-Ar ages when thousands of grains are averaged.)
19. Because immature glauconies have thinner subgrain laminae, they would be most sensitive to Ar loss. According to a model of Ar recoil in thin parallel laminae (*9*), grains with thinner laminae also undergo greater ^{39}Ar recoil losses. Thus, if all the younger ages result from ^{40}Ar loss, they may be expected to be inversely correlated with their ^{39}Ar recoil loss. In the clay mineral illite, such a relation was attributed to low-temperature loss of both ^{39}Ar and ^{40}Ar from similar lattice sites [H. Dong, C. M. Hall, D. R. Peacor, A. N. Halliday, *Science* **267**, 355 (1995)]. In contrast, there is no simple relation between ^{39}Ar recoil and apparent age in the glaucony populations (Table 1).
20. Although this estimate is uncertain because of the difficulty in obtaining representative averages for small samples in heterogeneous populations, this method mitigates the extra uncertainties (that is, the 2% accuracy of the ^{40}Ar-^{39}Ar ages based on the age of flux monitors) involved in a comparison with the published bulk K-Ar determinations.
21. J. P. Morton and L. E. Long, *J. Sediment. Petrol.* **54**, 495 (1984).
22. B. U. Haq, J. Hardenbol, P. R. Vail, *Science* **235**, 1156 (1987). These curves were constructed according to the hypothesis that stratigraphic sequences are controlled primarily by changes in global sea level. Although this model has received much support [for instance, K. G. Miller *et al.*, *ibid.* **271**, 1092 (1996)], it has also encountered numerous challenges, particularly by F. M. Gradstein *et al.* [*ibid.* **241**, 599 (1988)], who pointed out that the stratigraphic uncertainties of the higher-frequency cycles (1 to 3 Ma) making up the seawater curves are currently too high to permit a test of whether they were globally synchronous.

23. We thank C. M. Hall and an anonymous reviewer for their constructive comments. Supported by an operating grant from the Natural Sciences and Engineering Research Council of Canada (D.Y.).

20 October 1997; accepted 29 January 1998

Distribution of *Thiobacillus ferrooxidans* and *Leptospirillum ferrooxidans*: Implications for Generation of Acid Mine Drainage

Matthew O. Schrenk, Katrina J. Edwards,* Robert M. Goodman, Robert J. Hamers, Jillian F. Banfield

Although *Thiobacillus ferrooxidans* and *Leptospirillum ferrooxidans* are widely considered to be the microorganisms that control the rate of generation of acid mine drainage, little is known about their natural distribution and abundance. Fluorescence in situ hybridization studies showed that at Iron Mountain, California, *T. ferrooxidans* occurs in peripheral slime-based communities (at pH over 1.3 and temperature under 30°C) but not in important subsurface acid-forming environments (pH 0.3 to 0.7, temperature 30° to 50°C). *Leptospirillum ferrooxidans* is abundant in slimes and as a planktonic organism in environments with lower pH. *Thiobacillus ferrooxidans* affects the precipitation of ferric iron solids but plays a limited role in acid generation, and neither species controls direct catalysis at low pH at this site.

A fundamental component of the sulfur geochemical cycle is the release of sulfate into solution through oxidative dissolution of sulfide minerals. Because sulfides are at least a minor component of most rocks, this process is almost ubiquitous in chemical weathering. Weathering of sulfide-rich rocks with low neutralization capacity forms sulfuric acid–rich solutions that can carry high metal loads. When ore bodies are exposed by mining, this results in an environmental condition known as acid mine drainage (AMD).

Pyrite (FeS_2) is the most abundant sulfide mineral in Earth's crust. Exposure of pyrite surfaces to oxygen and water results in the formation of sulfuric acid. Ferric iron, an abundant alternative electron acceptor in many AMD solutions, interacts effectively with surface sulfur species (*1*) and pro-

M. O Schrenk and K. J. Edwards, Department of Geology and Geophysics, University of Wisconsin–Madison, 1215 West Dayton Street, Madison, WI 53706, USA.
R. M. Goodman, Department of Plant Pathology, University of Wisconsin–Madison, 1630 Linden Drive, Madison, WI 53706, USA.
R. J. Hamers, Department of Chemistry, University of Wisconsin–Madison, 1101 University Avenue, Madison, WI 53706, USA.
J. F. Banfield, Department of Geology and Geophysics, University of Wisconsin–Madison, 1215 West Dayton Street, Madison, WI 53706, USA.

*To whom correspondence should be addressed. E-mail: katrina@geology.wisc.edu